ChemElectroChem

Review
doi.org/10.1002/celc.202300621

Chemistry Europe
European Chemical Societies Publishing

www.chemelectrochem.org

Intelligent Nano-Colloidal Electrolytes for Stabilizing Lithium Metal Anodes: A Review

Minhong Lim,[a] Jiyeon Seo,[a] Bokyung Choi,[a] Beomjun Kim,[a] Jiwon Lee,[a] Sanghyun Park,[a] and Hongkyung Lee*[a, b]

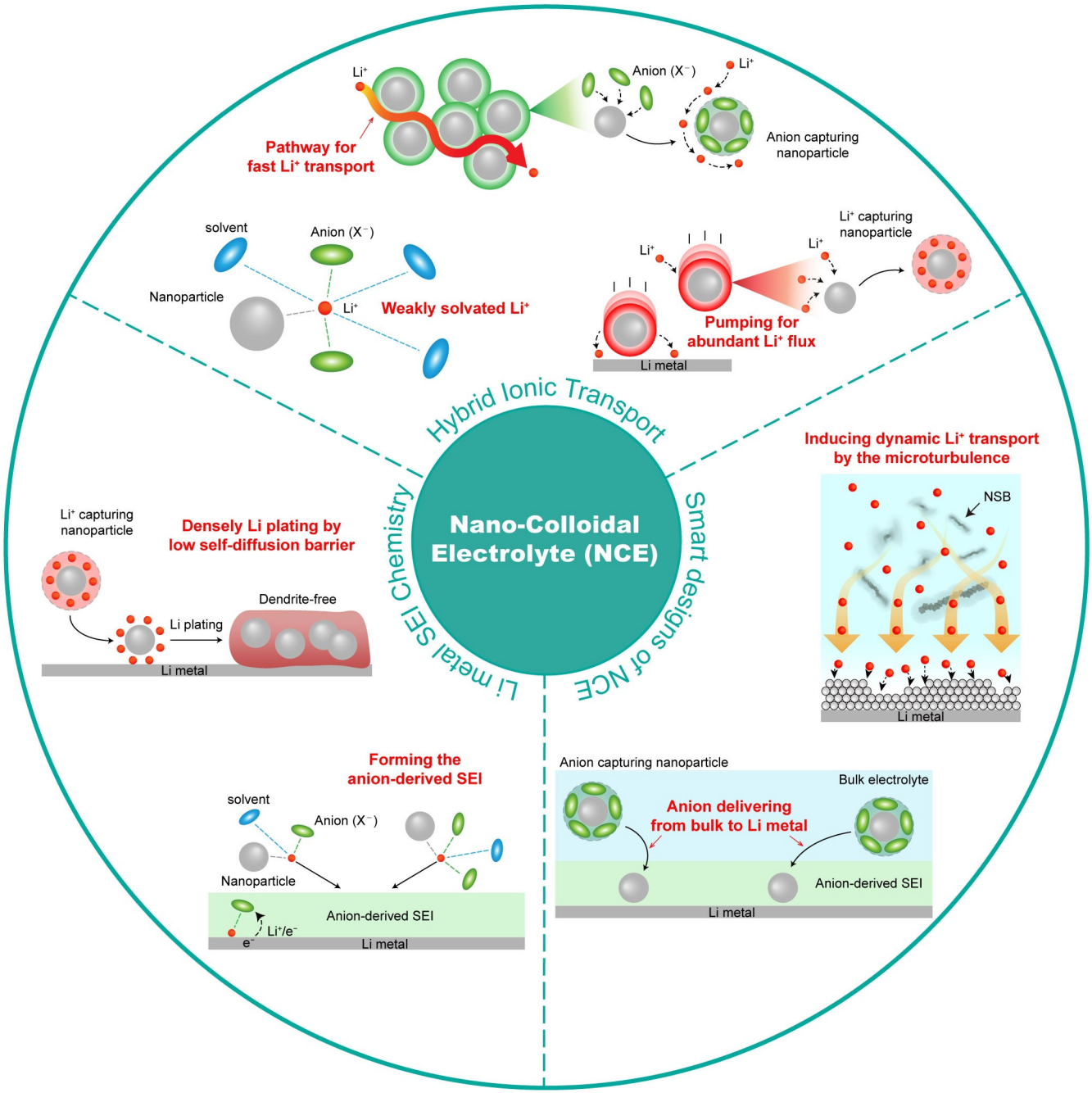

Although Li-metal has been revisited as the most attractive anode in building high-energy-density batteries owing to its superiority, such as ultimate theoretical capacity and lowest working voltage, notorious Li dendrite growth has plagued its practical uses. Since dendritic Li electroplating is mostly caused by poor Li^+ transport and inferior stability of solid-electrolyte interphase (SEI), an innovative reframing of the electrolyte is crucial to the success of Li-metal anodes (LMAs). This review presents a new class of electrolytes, nano-colloidal electrolytes (NCEs), providing a new avenue for next-generation Li-metal batteries (LMBs). Without searching for new salts/solvents or their compositional tuning, NCEs exploiting multi-functional nanoparticles dispersed in liquid electrolytes can promote Li^+ transport and reinforce the SEI of liquid electrolytes that are solely used. This review discusses various types of nanoparticles and their key roles in demonstrating excellent suppression of Li dendrite growth and enhancing the cycling stability of LMBs. Unraveling the underlying design principles of NCEs offers practical solutions for stabilizing LMAs, paving the way for developing intelligent battery systems.

1. Introduction

The demand for reliable and efficient electrochemical storage systems has become increasingly critical with the rapid growth in the sales of electric vehicles (EVs) and electronic devices worldwide. In particular, Li-ion batteries (LIBs), one of the most energy-dense battery platforms, are typically used as energy sources in EVs.[1–3] However, graphite, used as a commercial anode material in LIBs, has hit walls in terms of enhancing the energy density per volume and weight. Li metal anodes (LMAs) are the ideal candidate for next-generation anode materials to replace graphite anodes due to their higher theoretical capacity (graphite: 372 mAh g^{-1} vs. Li metal: 3860 mAh g^{-1}) and lowest redox potential (−3.04 V vs. SHE).[4–8] Despite these advantages, some challenges are associated with using LMAs, such as forming Li dendrites, which can reduce the cycle life and safety of Li metal batteries (LMBs).[9–12]

Li dendrite formation could deteriorate owing to poor Li^+ transport and the solid-electrolyte interphase (SEI) derived from the electrolyte composition. There are two main theories related to the formation of Li dendrite growth: slow Li^+ transport and the weaker modulus of the SEI.[13–15] Chazalviel provided insights into Li metal dendrite formation using the Sand time equation, which considers the bulk Li^+ concentration, current density, apparent diffusivity, and Li^+ transference number (t_{Li+}).[13,14] This equation indicates that the transition from mossy to dendritic Li morphology occurs near the LMA surface at zero Sand time, and this transformation is more pronounced at higher current densities and lower apparent diffusivities, bulk concentrations, and t_{Li+}. In addition, Newman suggested that the value of shear strength for mechanically suppressing Li dendrites is about the shear modulus of Li metal (3.4 GPa).[15] In fact, the presence of a preformed SEI on the Li metal surface can inhibit Li penetration owing to its higher mechanical strength, assuming that it has a shear modulus approximately twice that of Li metal (>6.8 GPa). To prevent Li dendrite formation by controlling SEI modification, forming a physically rigid SEI, such as fluorinated-enriched and anion-derived materials, is crucial. These theories about suppressing the dendritic Li morphology during cell cycling are convincing for the application of LMBs.

Numerous studies have addressed the challenges associated with deficient Li^+ transport and SEI formation contributing to LMB degradation. These strategies include (1) separator coating with inorganic materials by adsorbing the anion, inducing high t_{Li+},[16–18] (2) LMAs surface pretreatment before cell cycling to form a rigid SEI,[11,19–21] and (3) a protective layer as an artificial SEI for enhanced mechanical strength.[22–27] Researchers have actively explored electrolyte reconstruction by altering the salt/solvent composition to modulate the Li^+ transport mechanism and SEI chemistry.

In response to the limitations identified in previous research, significant advancements have been made in the electrolyte composition of LMBs, driven by the pursuit of addressing the challenges and meeting specific scientific and technological requirements.[28–30] First, various additives were added to the conventional electrolyte to reinforce the SEI with additive-derived components.[31–34] Fluoroethylene carbonate (FEC) and lithium nitrate ($LiNO_3$) are typically used as additives in carbonate-based electrolytes to form lithium fluoride (LiF) and lithium nitride (Li_3N), respectively. Such methodologies have been shown to reinforce the SEI of LMAs, enhancing their Coulombic Efficiency (CE). However, carbonate-based electrolytes are more incompatible with LMAs than ether-based electrolytes.[35,36] Despite the poor oxidation stability attributed to the high highest occupied molecular orbital (HOMO) level of ether solvents, numerous studies have been conducted to explore the use of ether-based electrolytes, such as high-concentration electrolytes (HCEs), with high concentrations of Li salts.[36] This electrolyte exhibits a densely plated Li morphology and facilitates anion-derived SEI formation owing to the strong interaction between Li^+ ions and anions, leading to a high CE of approximately 99%. However, HCEs suffer from high electrolyte viscosity, which is why they have low ionic conductivity. This can be overcome using a diluent. Because the diluents only interact with the solvent, localized high-concentration electro-

[a] M. Lim, J. Seo, B. Choi, B. Kim, J. Lee, S. Park, Prof. Dr. H. Lee
Department of Energy Science & Engineering
Daegu Gyeongbuk Institute of Science and Technology (DGIST)
333 Techno Jungang-daero, Hyeonpung-eup, Dalseong-gun, Daegu 42988, Republic of Korea
E-mail: hongkyung.lee@dgist.ac.kr
[b] Prof. Dr. H. Lee
Energy Science and Engineering Research Center
Daegu Gyeongbuk Institute of Science and Technology (DGIST)
333 Techno Jungang-daero, Hyeonpung-eup, Dalseong-gun, Daegu 42988, Republic of Korea

lytes (LHCEs) show a similar solvation structure shell to HCE, leading to high oxidation stability.[35,37] Recently, a weakly solvating electrolyte (WSE) with a potentially weaker solvating solvent was used to induce contact ion pairs (CIP) and aggregates (AGG) without a diluent.[38–41] LHCE and WSE showed superior CE, high ionic conductivities, and stable SEI. Despite these efforts, some problems still exist, such as poor Li^+ transport, high cost due to excessive salt use, and short persistence of the SEI modification effect, resulting in Li dendrites and poor cycle stability of LMBs.

Recently, nano-colloidal electrolytes (NCEs), in which nanoparticles are dispersed in a liquid electrolyte, have been highlighted as a solution to overcome the liquid electrolyte problem, which involves poor/non-uniform Li^+ transport,[42,43] high cost of Li salts,[44] and weak shear modulus of the electrolyte-derived SEI.[45] NCEs present a new paradigm for improving the Li^+ transport characteristics and interfacial stability, which are highly dependent on the type of electrolyte. The liquid electrolytes used in Li secondary batteries generally contain salts, organic solvents, and other additives. The combination of salts/organic solvents, which account for most electrolytes, determines most electrolyte characteristics. Therefore, the strategy to enhance Li^+ transport and interface properties using only the salt/solvent combination of the electrolyte has limitations, and the control of the SEI composition and mechanical strength formed by electrochemical reactions is minimal. For example, although the inorganic material content should be increased to enhance the mechanical properties of the interface, it is unreasonable to increase the content of a specific material using only the salt/solvent composition.[46] On the other hand, NCEs can participate in the Li solvation structure of the electrolyte and the interfacial reaction of the electrode to modify Li^+ transport and increase the inorganic content at the interface.

Minhong Lim completed his B.S. degree in undergraduate studies in 2020. He is currently an M.S. & Ph.D. integrated student at the Department of Energy Science and Engineering at DGIST, under the supervision of Prof. Hongkyung Lee. His research interests include the applications of nanoparticles designed for liquid electrolytes and the analysis of Li nucleation and growth mechanisms to suppress dendrite formation in Li metal batteries.

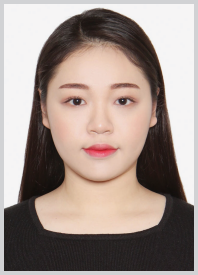

Jiyeon Seo completed her B.S. degree in Nanotechnology and Advanced Materials Engineering at Sejong University in 2021. She is currently an M.S. & Ph.D. integrated student at the Department of Energy Science and Engineering at DGIST, under the supervision of Prof. Hongkyung Lee. Her research interests include inhibiting dendrite growth by surface modification of Li metal anode in Li metal batteries and modification of Cu current collector in anode-free Li metal batteries.

Bokyung Choi completed her B.S. degree in chemical engineering and applied chemistry at Chungnam National University in 2021 and is currently an M.S. student at the Department of Energy Science and Engineering at DGIST. Her research focuses on the design of a protection layer for Li-S batteries.

Beomjun Kim completed his B.S. in undergraduate studies at Kwangwoon University in 2023 and is currently an M.S. & Ph.D. integrated student in the Department of Energy Science and Engineering at DGIST, under the supervision of Prof. Hongkyung Lee. His research interests include the photothermal and chemical surface treatments of Li metal anode.

Jiwon Lee completed his B.S. in undergraduate studies at DGIST in 2022 and is currently a graduate research assistant in the Department of Energy Science and Engineering at DGIST, under the supervision of Prof. Hongkyung Lee. His research focuses on cell-level pressure evolution analyses and modification of current collector for Li metal battery.

Sanghyeon Park completed his B.S. degree in polymer engineering at Kyoungpook National University in 2022 and is currently an M.S. student at the Daegu Gyeongbuk Institute of Science and Technology. His research interests include the physical and chemical surface treatments of Li metal anode.

Hongkyung Lee is an associate professor in Department of Energy Science and Engineering at DGIST. He obtained his Ph.D. in Chemical and Biomolecular Engineering from KAIST, South Korea, in 2016. His Ph.D. research has focused on electrochemical interfaces in Li-air batteries and core technologies for Li metal stabilization. He then worked as a postdoctoral research associate at the Pacific Northwest National Laboratory (PNNL) from to 2017–2019, where he contributed to the Battery500 consortium by advancing Li metal stabilization through multi-scale interface engineering. His current research interests include dendrite-free electroplating of high-capacity metallic anodes, fast-charging Li ions, and real-time diagnosis of battery failure.

This review aims to provide an understanding of NCE with working principles, recent progress, and the roles of materials and design principles in modifying traditional electrolytes. First, we suggest the concepts and structure of the construction of NCEs and the principles of effectively modulating the Li^+ environment and Li surface chemistry. NCEs are liquid electrolytes with dispersed inorganic nano-materials that allow interactions between the inorganic nanoparticle and electrolyte species. The role of NCEs can vary based on the characteristics of nanoparticles, such as body material, functional groups, size, and dimensions. In addition, this paper defines the key roles of NCEs and their working principles based on recent research findings that inhibit Li dendrite formation with various NCEs. Finally, this review presents our perspectives and design principles for advancing the NCE. Further elaboration on this topic is provided in the following section.

2. Concepts and Structures

NCEs are composed of liquid electrolytes and dispersed nanoparticles, considered organic/inorganic hybrid electrolytes. The most common form of a hybrid electrolyte is the ceramic/polymer composite electrolyte (solid-in-polymer), in which ceramic nanoparticles are introduced to lower the crystallinity of the polymer and increase the mobility of Li^+ to improve its ionic conductivity of the polymer electrolyte.[47–50] However, the NCEs discussed in this study have a form in which nanoparticles are dispersed in a liquid electrolyte (solid-in-liquid) and are hybrid electrolytes based on a different concept from conventional ceramic/polymer composite electrolytes. Nanoparticles can move freely in the NCE with Li^+ or anions via Brownian motion, and it is possible to control Li^+ transport paths or partially participate in the interphase.[51,52] Therefore, we can design the body materials and functional groups of nanoparticles to fulfill specific roles tailored to our purposes.

In general, Li^+ transport and SEI characteristics in electrolytes are determined by their composition, such as the types of salts and solvents and their concentrations. However, because nanoparticles can intervene in the Li^+ microenvironment, the NCE independently changes the degree of coordinated Li^+ and composition of SEI, allowing for the design of new electrolyte structures distinct from existing design principles. This is similar to the case of meltable additives, which can improve the composition and structure of the SEI by inducing specific electrochemical reactions. However, it is difficult to predict the chemical/electrochemical reaction pathways at the interface. In contrast, nanoparticles can effectively enhance physical properties by directly participating in SEI formation reactions through precipitation.

Various materials have been used in NCEs to suppress Li dendrite formation by modulating the Li^+ microenvironment. Oxide- and nitride-based nanoparticles can capture anions by hydrogen bonding and Lewis acid-base interactions between acidic functional groups and nanoparticles, selectively increasing Li^+ transport for high t_{Li+}. In addition, the anion-capturing effect depends on the type of functional groups, such as hydroxyl, citric acid, amine, and sulfonic acid. Metal-organic frameworks (MOFs) can capture anions through open metal site absorption, enabling Li^+ transport with low activation energy. On the other hand, some nanoparticles that could interact with Li^+ induced weakly solvated Li^+, forming a contact ion pair (CIP) and aggregate (AGG), and Li^+ was pumped toward the LMAs surface for abundant Li^+ concentration. In this case, the SEI chemistry can be modified with anion-derived compounds through the dominantly decomposed anion, owing to the lower lowest unoccupied molecular orbital (LUMO) in the CIP and AGG solvation structures.

The dispersion property of nanoparticles may be strongly linked to the enhanced interaction between nanoparticles and electrolyte species, which helps prevent the particles from coming into close contact. Thus, the nanoparticle could be well-dispersed through the dominant coordination between Li^+ or anions without aggregation,[52,53] depending on the type of material, shape, size, concentration, and surface functional groups of the nanoparticles.[53–58] It is beneficial to add a small amount of nanoparticles with a high BET or to design a functional group that can strongly bind to many electrolyte species. Although the acid group can facilitate the dispersion of nanoparticles to some extent, excessively high acidity may impede dispersion due to strong interactions among the nanoparticles. Nanoparticles could effectively interact with anions when regulating the size of an anion as well as the surface chemistry of the material. Therefore, it is crucial to understand the microstructure of the salt, solvent, and nanoparticles and use this understanding to establish design principles.

An NCE designed based on the considerations above can address problems that cannot be overcome by commercial liquid electrolytes and suppress Li dendrite formation (Figure 1). Li^+ transport and SEI modification in conventional electrolytes are limited to the salt and solvent. However, NCE allows performance tuning, even without differences in the electrolyte composition. The principles of Li^+ transport enhancement are (1) selective enhancement of Li^+ transport through anion absorption[59–63] and (2) increased accessibility of anions in the Li solvation shell by weakening the interactions between the solvent and Li^+.[52,64,65] Likewise, the principles of modifying the SEI are (1) utilization of the high binding energy and low self-diffusion barrier with Li^+ leading to uniform ion deposition;[66,67] (2) formation of a fluorinated compound-enriched SEI by co-depositing nanoparticles with anions or additives into the SEI, simultaneously inhibiting dendrites owing to their high rigidity;[63,68] and (3) SEI modification through highly soluble nanoparticles with superior components for the SEI.[52,69] Anion-derived compounds (e.g., $LiPF_6$, LiFSI) or inorganic materials (e.g., LiF, Li_3N) originate from delivered anions or soluble nanoparticles by electrochemical and chemical reactions, respectively. Recently, research has focused on granting smart functionality to nanoparticles, enabling them to act as nano-carriers for additives[51] or induce nano-convection,[70] thus inhibiting Li dendrite formation. The details are presented in the next section.

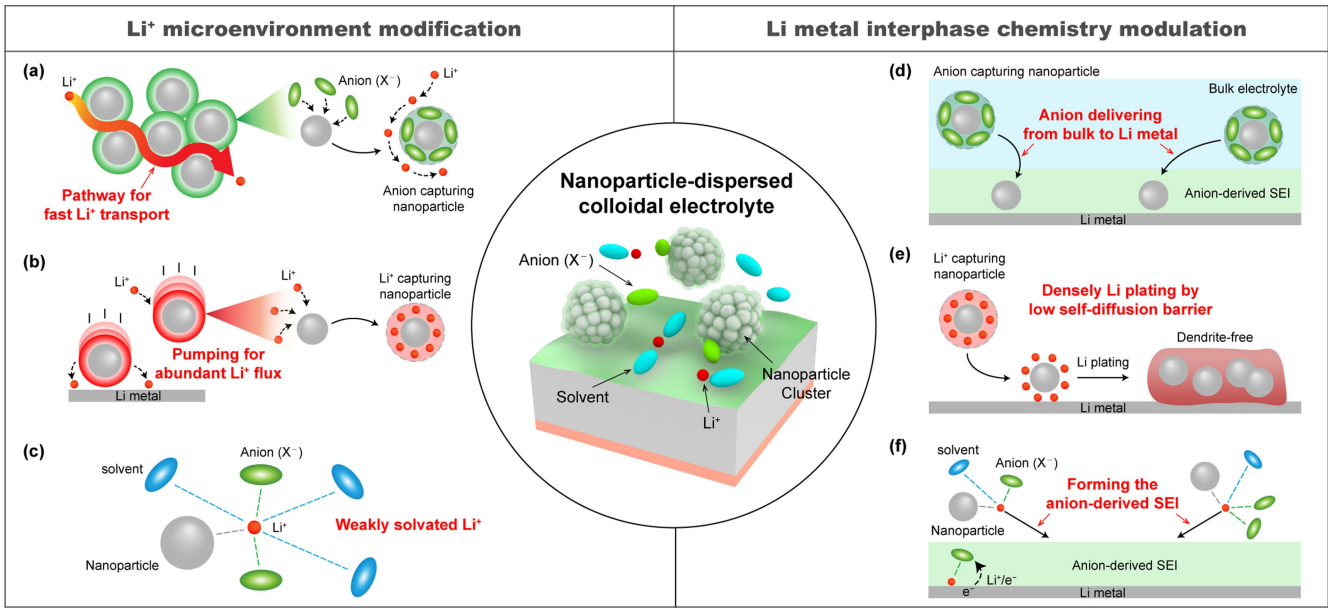

Figure 1. Diagrams of the solvation structures and various roles of NCEs. (a) Anion absorbing nanoparticle forming a pathway for fast Li^+ transport (b) Pumping for abundant Li^+ flux near the LMA surface with Li^+ capturing nanoparticle (c) Inducing strong interaction between Li^+ and anion by weakly solvated Li^+ (d) Anion delivering toward LI metal forming anion-derived and nanoparticle co-deposited SEI (e) Pumped Li^+ could densely deposited along the nanoparticle surface by low self-diffusion barrier (f) Forming the anion-derived SEI through the weakly solvated Li^+.

3. Modulation of Li^+ microenvironment

The formation of Li dendrites is strongly linked to the Li^+ solvation structure, which influences the rapid and uniform Li^+ flux toward the LMAs and leads to alterations in the anion and solvent behaviors and the selection of SEI components.[71,72] Achieving uniform and rapid Li^+ transport is crucial for preventing sporadic Li plating by tuning the Li nucleation and growth mode to the instantaneous nucleation mode. Despite various attempts to enhance Li^+ transport,[43,73,74] NCE approaches have emerged as semi-permanent methods for redistributing the Li^+ flux throughout an extended cycle life. In addition, some NCEs establish strong interactions between Li^+ and the anions, reinforcing the Li-metal interface. NCE approaches can tune the SEI without restraints and change the salt/solvent composition of the blank electrolytes. In the following section, we discuss these distinct types of NCEs based on their specific characteristics.

3.1. Improving transference number (t_{Li+})

Improving the ionic conductivity helps reduce the overpotential in electrolytes and improves capacity retention rates by enhancing the space charge and uniformity of the Li^+ flux during the battery cycle process. Most nanoparticles physically hinder ion transport when dispersed at high concentrations in the NCE, and the overall cell cycling performance can deteriorate owing to decreased ionic conductivity. However, although the ionic conductivity decreases, the selective Li^+ ionic conductivity can still be enhanced due to the improvement in t_{Li+}, thereby ensuring good battery performance.[51,62] As shown in the formula below, the t_{Li+} is the relative mobility of the cations (u_{Li+}) compared to the mobility of anions carriers (u_{x-}).

$$t_{Li^+} = \frac{u_{Li^+}}{u_{Li^+} + u_{X^-}}$$

Many studies have been conducted to improve the t_{Li+} of electrolytes using NCEs, and material and functional group selection is important for obtaining superior Li^+ transport in NCEs. As an example, Lu's group improved battery performance by creating NCE based on porous MOF particles dispersed in 1 M lithium hexafluorophosphate ($LiPF_6$) in ethylene carbonate (EC)/diethyl carbonate (DEC) commercial electrolyte at concentrations of 125 and 250 mg mL^{-1}, which was named MLE-1 and MLE-2 (Figure 2a).[59] Compared to the blank electrolyte, the ionic conductivities of MLE-1 and MLE-2 were reduced by 25% and 60% at each concentration. However, their transference numbers improved, reaching 0.57 and 0.61 from 0.3, which was the value of the blank electrolyte (Figure 2b). Given that the high effective Li^+ ion conductivity ($\sigma_{eff} = \sigma_{bulk} \times t_{Li+}$), the transport properties of the Li^+ ions may increase, and the decrease in the measured ionic conductivity can be overcome by high t_{Li+}.[75,76] Furthermore, improving t_{Li+} is vital for suppressing dendrite growth, a problem in next-generation LMBs (Figure 2c, d). Therefore, it is an important physical property in the design of colloidal electrolytes.

In addition, there have been reports of t_{Li+} improvements in studies on NCE based on boron nitride nanosheet (BNNS) by Huang's group at Wuhan University.[60] In particular, when the NH_2 functional group was added to the BNNS through a synthesis method using urea, the acidity of the boron atoms was improved, and the mobility of the anions was reduced

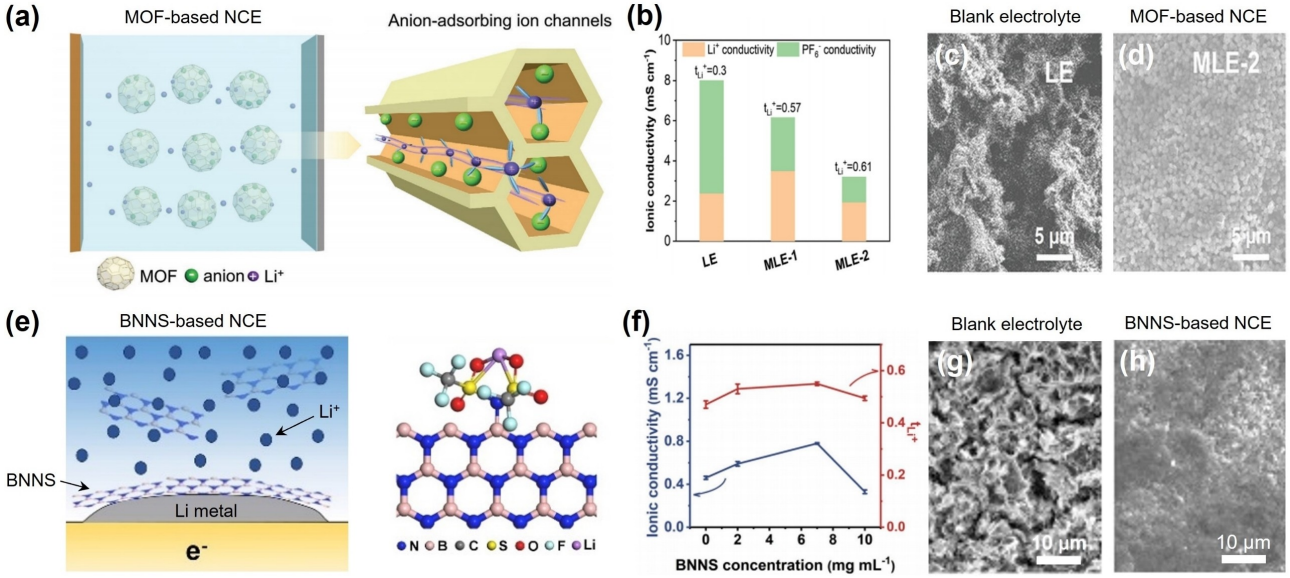

Figure 2. (a) Scheme of MOF-based NCE that adsorb anion-forming ion channels. (b) Comparison of effective Li ionic conductivity in blank electrolytes MLE-1 and MLEL-2. Reproduced from[59] Copyright (2020), with permission from Wiley-VCH. (c, d) SEM image of the electrodeposited Li metal morphology obtained from the Li||Li cell after the 150th cycle. (e) Scheme of Li dendrite suppression using BNNS-based NCE containing BNNS with NH_2 functional groups. (f) t_{Li+} and ionic conductivity values of blank and NCE. (g, h) Electroplating morphology of Li metal obtained from the Li||Cu cell after cycling. Reproduced from[60] Copyright (2020), with permission from Elsevier.

(Figure 2e). In a colloidal electrolyte where the BNNS particles were dispersed in 1 M lithium bis(trifluoromethanesulfonyl)imide (LiTFSI) in 1,3-dioxolane (DOL)/dimethoxyethane (DME) + 2 wt% $LiNO_3$ at a concentration of 7.0 mg mL^{-1}, a t_{Li+} value of 0.55 was achieved (Figure 2f). This was an improvement over that of the blank electrolyte (0.47). As previously mentioned, the boron atoms of the BNNS reduced the anions' mobility and enhanced the t_{Li+} through a Lewis acid-base reaction with the N atoms of the $TFSI^-$. Consequently, the concentration gradient in the electrolyte gradually increased, which led to a low overpotential during Li electrodeposition and induced an excellent rate performance. Moreover, BNNS demonstrated advantages in suppressing Li dendrites, which possess a 3.4 GPa shear modulus through its 2-dimensional structure and a high shear modulus of approximately 950 GPa (Figures 2g and h).

3.2. Reducing the Li^+ solvation power

In the NCE, nanoparticles can directly bind to Li^+ instead of adsorbing anions, thereby modifying the Li^+ solvation structure. At that time, a weakly solvating structure was formed, inducing a strong interaction between the anions and Li^+ owing to the nanoparticles existing close to the solvated Li^+. Unlike prior studies that focused on enhancing t_{Li+} by controlling the mobility of anions, this approach effectively suppresses Li dendrite formation by reinforcing the SEI with anion-derived compounds.

Recently, the use of Li_2O nanoparticles as inorganic additives in NCEs has been proposed, wherein their role involves interaction with Li^+ to displace the solvent from the primary solvation shell (Figures 3a and b).[52] Kim et al. demonstrate the feasibility of solvation structure modulation near the Li_2O nanoparticles by MD simulations of molecules (Li^+, PF_6^-, FEC, EC, and DEC). The fluorinated species can closely pack Li^+, whereas other solvent molecules are positioned far from the core ions. This modulation occurred exclusively close to the Li_2O nanoparticles and did not influence the areas further away from the Li_2O nanoparticles. If the dispersity is poor during Li plating, the Li morphology might show a dendritic shape rather than a blank electrolyte owing to the lower ionic conductivity. Therefore, it is crucial to maintain a nanosized structure for proper dispersion within the NCE, as this dispersion is critical to the formation of an inorganic-enriched SEI. Indeed, as shown in Figures 3 c and d, the Li_2O-based electrolyte shows a particle-like Li morphology, whereas the blank electrolyte exhibits a Li filament shape.

In addition, the potential of the Li_3N nanoparticles as nanofillers in NCEs was investigated. Recently, Cui et al. explored the utilization of Li_3N nanoparticles in NCEs and revealed a mechanism similar to that of Li_2O-based NCEs (Figure 3e).[64] Notably, the Li_3N nanoparticles exhibited the ability to lower the ratio of Li^+ coordinated with EC compared to free EC, thereby promoting the formation of a stable SEI with an organic-poor composition. By tightly arranging fluorinated species and anions around Li^+ and maintaining a distinct separation from other solvent molecules, Li_3N nanoparticles inhibit dendritic growth. As shown in Figures 3f and g, Li_3N-based NCE showed compact Li deposition morphology, demonstrating the potential of these inorganic additives to improve the performance of LMBs.

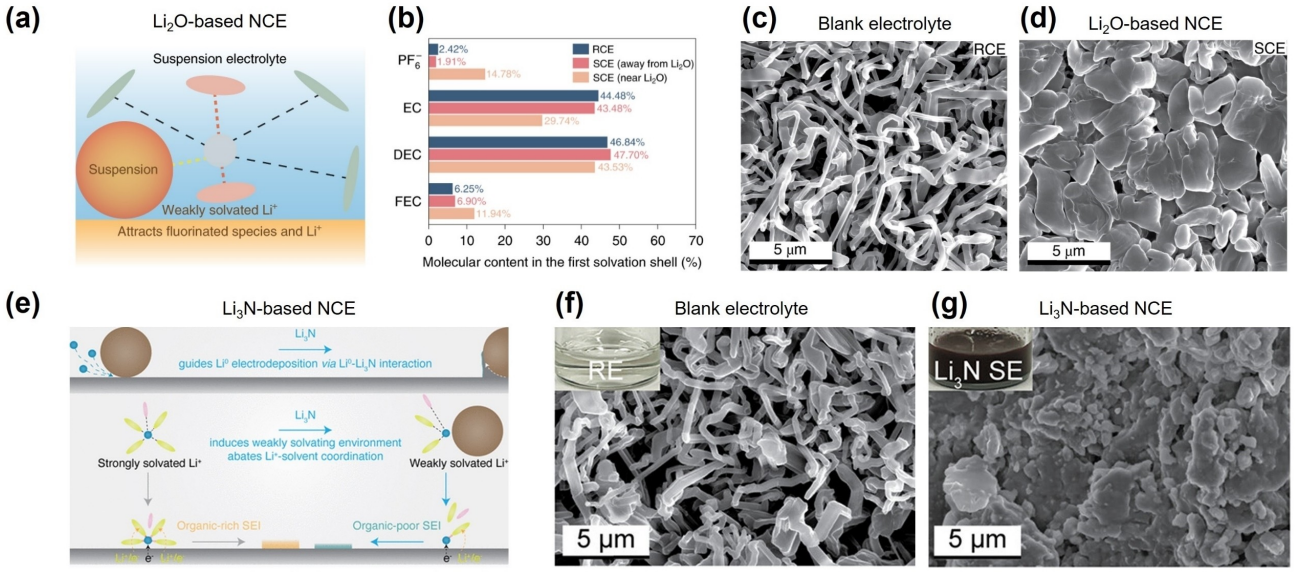

Figure 3. Schemes involving NCEs establishing a weakly solvated Li microenvironment for enriched CIP and AGG ratio. (a, b) Electrolyte species content in the first Li^+ solvation shell in the blank electrolyte and away from and near the Li_2O slab of NCE. SEM images of plated Li obtained from Li||Cu cells were deposited at 1 mA cm^{-2} and 1 mAh cm^{-2} using (c) blank electrolyte and (d) Li_2O-based NCE. Reproduced from[52] Copyright (2022), with permission from Springer Nature. (e) Initiating a weakly solvated environment that abates the Li^+-solvent coordination, forming an SEI enriched with inorganic components. (f, g) SEM images of the electrodeposited Li metal morphology obtained from the Li||Cu cell. Reproduced from[64] Copyright (2023), with permission from American Chemical Society.

4. Modulating the Interface Chemistry

A poor SEI can induce uneven Li nucleation and growth, leading to the formation of Li dendrite.[77–79] Additionally, this could lead to less contact between the plated Li and the substrate Li, forming dead Li[80] and subsequently decreasing battery performance. Much research on modulating the SEI of Li metal has been actively conducted, inhibiting the problem caused by unevenly formed SEI.[81–84] Most previous studies on SEI modification have focused on tuning the electrolyte composition or pretreatment using the manufactured Li metal. Despite these efforts, some issues remain, such as unestimated parasitic reactions and cost-related challenges.[85–89] NCEs can modulate the interface chemistry, resulting in a surface enriched with fluorinated components and a low self-diffusion barrier without altering the electrolyte composition. In the following section, we introduce various NCEs, each possessing unique properties that enable SEI modulation.

4.1. Reduction of self-diffusion barrier

In addition to suppressing Li dendrites by improving the Li^+ transport properties, there have been studies that modulate the SEI using co-precipitated nanoparticles with Li^+ or anions to induce uniform Li electrodeposition. A joint research group from Tsinghua University and Drexel University conducted a study using a colloidal electrolyte with dispersed nanodiamonds and reported that dendrite growth could be suppressed by electrodepositing nanoparticles simultaneously with Li^+ (Figure 4a).[66] In a one-dimensional computational simulation, Li ions were adsorbed onto a nanodiamond surface with a low self-diffusion coefficient. By electrodepositing these materials together, the study identified a dense electroplated Li morphology was obtained. The primary role of the nanodiamonds can be divided into four stages. (1) Li^+ is adsorbed onto the nanodiamonds, which have a larger surface area and higher bonding force than the Cu current collector. (2) The nanodiamonds with adsorbed Li^+ moved near the Cu current collector due to electrical movement. (3) The nanodiamonds contributed to the uniform initial Li nucleation. (4) Li was electrodeposited with a small crystal size owing to the small size of the nanodiamonds, and Li had a uniform electrodeposition shape (Figures 4 b and c). However, even though the possibility of dendrite suppression has been realized, diamond nanoparticles are more difficult to mass-produce than other types of nanoparticles and have poor price competitiveness. However, these issues need to be addressed.

Additionally, Chen et al. published the results of a study that used inorganic nanoparticles with a good affinity for Li to suppress Li^+ depletion at the electrode interface and induce uniform Li electrodeposition as a result. The large surface area and adsorption capacity of Montmorillonite (MMT) that was dispersed in the electrolyte were used to elicit a "self-concentration" phenomenon that raised the Li^+ concentration on the nanoparticle surfaces, and this allowed for a greater amount of Li^+ transport (Figure 4d).[67] The ion depletion time at the electrode interface, that is, the sand time, was delayed by a large amount of Li^+ transport, which suppressed the non-uniform electrodeposition of Li ions in the blank electrode. In addition, because MMT particles have a low self-diffusion coefficient, they induce Li to grow uniformly along the particle

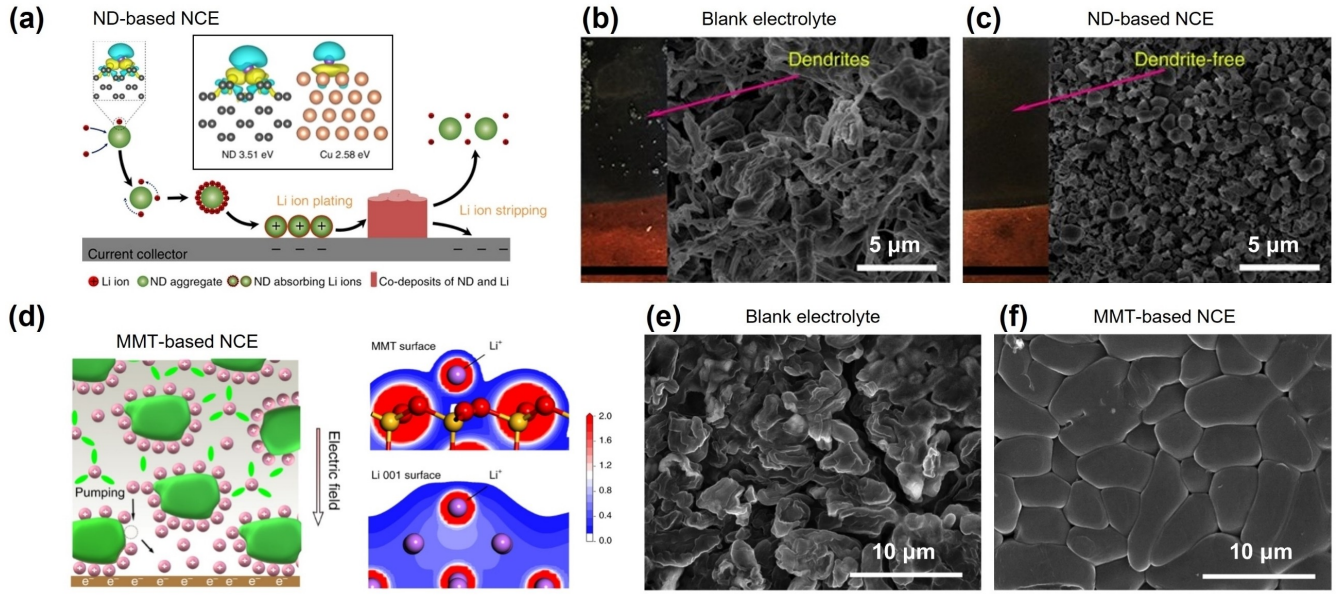

Figure 4. (a) Diagram of the dendrite suppression mechanism of nanodiamonds in the electrolyte. (b, c) Top SEM images of Li morphology obtained from Li||Cu cells using Blank and ND-based NCE. Reproduced from[66] Copyright (2017), with permission from Springer Nature. (d) Scheme of the MMT particle mechanism in NCE. Li electrodeposited SEM images using (e) conventional liquid electrolyte and (f) MMT particle contained NCE. Reproduced from[67] Copyright (2020), with permission from Springer Nature.

surfaces. In practice, dendrites were suppressed by the shape of the electrodeposited Li morphology compared to the blank electrolyte at 0.5 mA cm^{-2} and 1.0 mAh cm^{-2} (Figures 4e and f). Given that the high ion adsorption capacity and low Li^+ diffusion barrier of the LMA surface are effective in suppressing dendrites, this is suggested as a standard for selecting nanomaterials to suppress Li dendrites.

4.2. Formation of fluorinated SEI

Previous studies have shown that nanoparticles dispersed in an electrolyte can co-precipitate on an electrode surface during battery operation. They can significantly affect the density of the Li plating based on the binding energy and self-diffusion barrier of the nanoparticles. However, several studies have used fluorinated compound-enriched SEI to secure rigid properties.

Some studies have examined HF generation due to $LiPF_6$ salt and trace amounts of moisture for modulating the SEI. This HF generation can initiate chemical reactions such as SiO_2 etching and contribute to hydrolysis reactions near the interface, which can transport reaction byproducts into the Li SEI component. (Reactions 1 and 2).[90,91]

$$LiPF_6 + H_2O \rightarrow POF_3 + 2HF + LiF \downarrow \quad (1)$$

$$SiO_2 + 4HF \rightarrow SiF_4 + 2H_2O \quad (2)$$

These side reactions led to the consumption of Li ions. However, a joint research team at Pacific Northwest National Laboratory and South Korea reported that it is possible to suppress Li dendrites and stabilize the surface by changing the components of the SEI.[63] When a SiO_2-based NCE was used in the LMB, the participation of SiO_2 in the interphase reactions promoted the formation of LiF on the SEI, and the reactivity of Li with HF could be controlled by increasing the amount of high-strength ceramic components such as fluorosilicate (Figure 5a). The specific reactions are shown below (Reactions 3 and 4). The XPS analysis results of the SEI that uses such an electrolyte confirmed that the LiF and $Li_xPO_yF_z$ peaks increased according to the SiO_2 content (>10 mg mL^{-1}), and increases in inorganic components in the SEI caused improvements in mechanical strength. Based on this effect, when SiO_2 was dispersed in an NCE at concentrations of 5.0 and 10 mg mL^{-1}, there was an effective dendrite growth suppression effect (Figures 5b and c).

$$SiF_4 + 2LiF \rightarrow Li_2SiF_6 \downarrow \quad (3)$$

$$Li_2SiF_6 + 8LiOH \rightarrow 6LiF \downarrow + Li_4SiO_4 \downarrow + 4H_2O \quad (4)$$

NCE using Al_2O_3 and SiO_2 as nanobeads were analyzed by Song's research team, who verified the effect of nanoparticles on the interface mechanical strength (Figure 5d).[68] In addition, nanoparticles deposited with Li ions chemically enhance the SEI properties, encouraging the outermost SEI layer shell (OSS) and SEI layers in the Li metal deposit to be LiF-rich. Better electrochemical performance was observed when the nanobead-based NCE was used compared to when Al_2O_3 was used at the same concentration. This was confirmed to be an effect of the SiO_2 nanoparticle network formed when small amounts of HF in the battery acted as a catalyst in the siloxane (–Si–O–Si–) formation reaction between the silane (–Si–OH) functional groups. Given this effect, it was confirmed that the

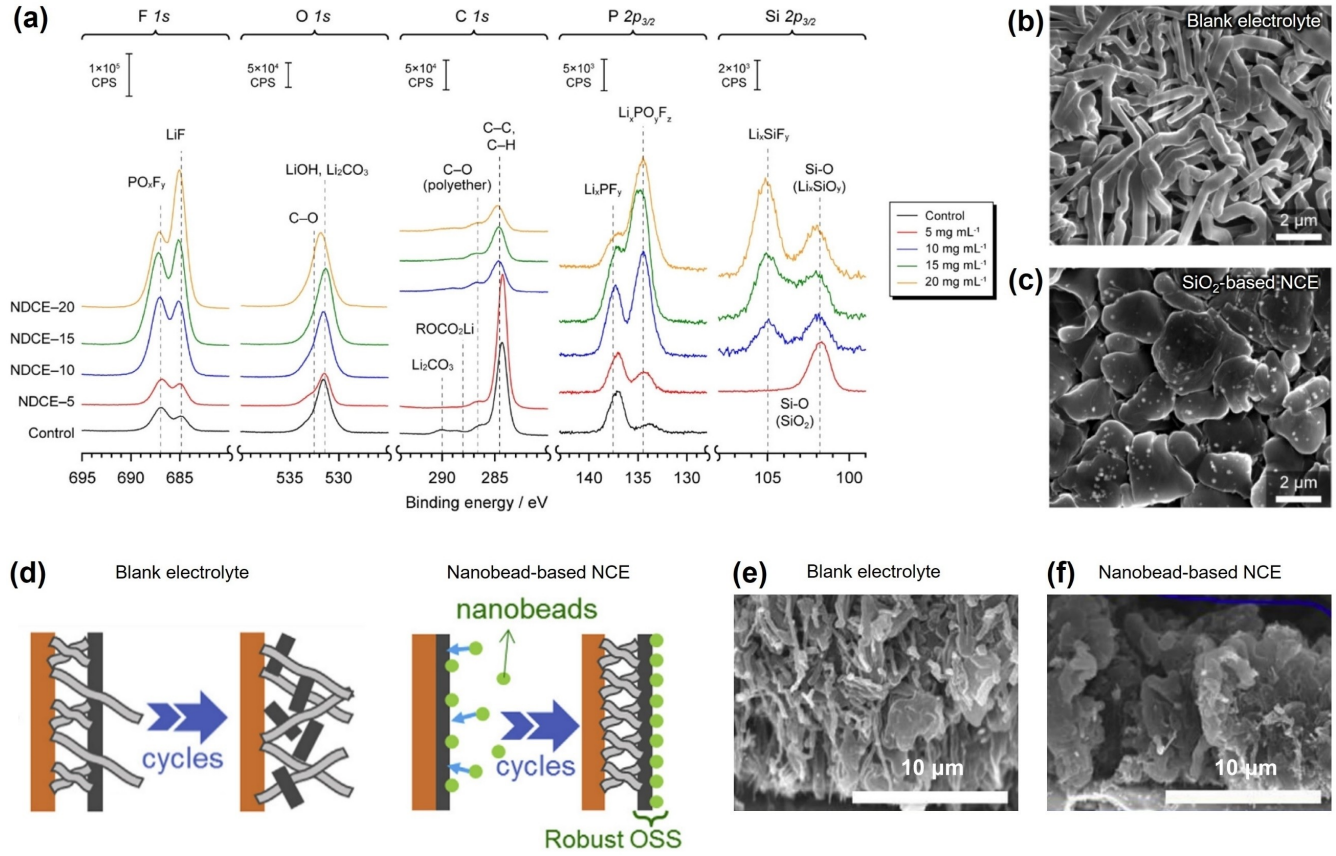

Figure 5. (a) XPS spectra of SiO_2-based NCE with 5 to 20 mg mL^{-1} and blank electrolyte. (b, c) SEM images of Li metal deposited morphology obtained from Li||Cu cells that operate using blank electrolyte and SiO_2-based NCE. Reproduced from[63] Copyright (2020), with permission from American Chemical Society. (d) The SEI modification scheme built by the nanobead-based NCE during the cycle. (e, f) Top view SEM images of blank electrolyte and nanobead-based NCE using Li||Cu asymmetric cells. Reproduced from[68] Copyright (2019), with permission from Elsevier.

morphology of the deposited Li was dense in the Li||Cu cells when the NCE was used (Figures 5 e and f).

4.3. SEI engineering utilizing partially soluble nanoparticles

Establishing a fluorine-rich compound-enriched SEI is crucial to suppressing dendrite formation effectively in LMBs. Based on this understanding, one approach for enhancing the SEI involves crafting NCEs with superior inorganic compounds as the constituent elements of the SEI. Indeed, given that many inorganic compounds are not readily soluble in the electrolyte, recent reports have highlighted their utilization in NCEs as dispersed nanoparticles to enhance the SEI properties.

Yao et al. proposed an NCE by fabricating LiF, a well-known LMA enhancer, in nanoboxes tailored for dispersion within an electrolyte.[69] These porous LiF nanoboxes exhibit exceptional dispersibility within the electrolyte matrix and resist precipitation. Their porous nature facilitates uniform Li^+ transport, mainly because of their potential interactions with the Li^+ ions within the electrolyte. Notably, the LiF nanoboxes underwent slight dissolution, enabling a fluoride-rich Li SEI formation (Figure 6a). This phenomenon was substantiated by TOF-SIMS analysis, which revealed an F-enriched composition of the SEI

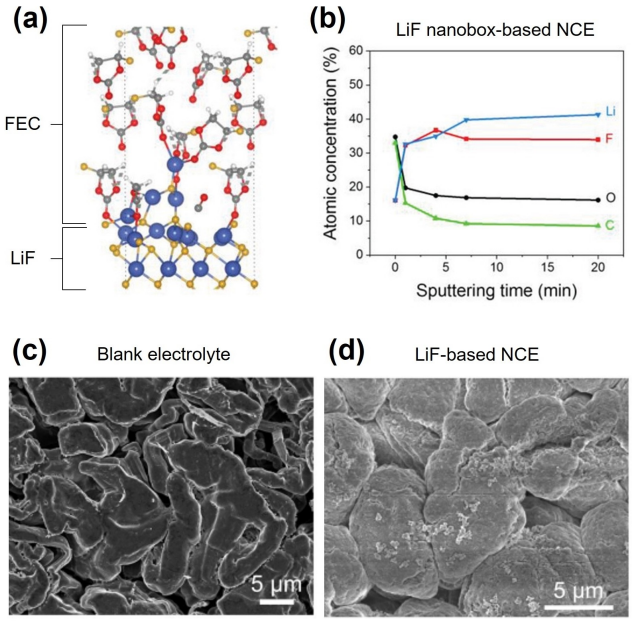

Figure 6. (a) Well-dissolute FEC by interaction between FEC and LiF in the electrolyte. (b) Fluorinated compound-enriched SEI that verified TOF-SIMS analysis. (c, d) SEM images of plated Li morphology obtained from Li||Li symmetric cell. Reproduced from[69] Copyright (2021), with permission from Wiley-VCH.

formed in the LMBs employing LiF nanobox-based NCEs (Figure 6b). Furthermore, the enhanced SEI contributes to the inhibition of Li dendrite formation. A comparative analysis of Li deposition morphologies was conducted using SEM for the blank electrolyte and the LiF nanobox-based NCE under current densities of 0.5 mA cm^{-2} and 5.0 mAh cm^{-2} (Figures 6 c and d).

5. Smart Functionality of Nanoparticles

As NCEs come into the spotlight, intelligent NCEs incorporating smart nanoparticles engineered for specific functionalities such as flame retardants,[92,93] convection-inducing materials,[70] and additive carriers[51] have emerged. Each NCE could suppress potential thermal incidents, induce microturbulence, and deliver additives toward the LMAs. Integrating these intelligent nanoparticles into NCEs not only revolutionizes battery performance but also refines battery safety.

5.1. Dynamic ion transport for Li dendrite suppression

Lim et al. reported a study aimed at modifying ion transport by remotely inducing mesoscale turbulence using external magnetic fields to achieve the magnetic properties of nanoparticles used in NCEs (Figure 7a).[70] Nanoparticles known as nanospinbars (NSBs) were fabricated by coating linearly arranged Fe_3O_4 with a SiO_2 outer layer. The SiO_2 outer layer inhibited parasitic reactions with the Fe_3O_4 core, electrolyte, and Li metal. The NSB-based NCE alleviated the significant ion concentration degradation observed in the blank electrolytes. Additionally, the localized ion depletion resulting from the non-uniform Li morphology can be overcome through NSB-assisted dynamic ion transport. In addition, the actuated uniform Li^+ transport via the NSBs rotation modified the Li nucleation and growth modes. Notably, the NSB-based NCE transitioned the 3D progressive mode of the blank to the 3D instantaneous mode through mesoscale turbulence, a transition validated through SEM images of deposited Li obtained from Li||Cu cells under conditions at 1.0 mA cm^{-1}, 1.0 mAh cm^{-1}. Unlike conventional electrolyte modification studies involving changes in the salt and solvent, NSBs can be used irrespective of the electrolyte composition. Indeed, NSBs induced uniform Li deposition regardless of the electrolyte type (carbonate-based, ether-based, or LHCE (Figures 7b–d).

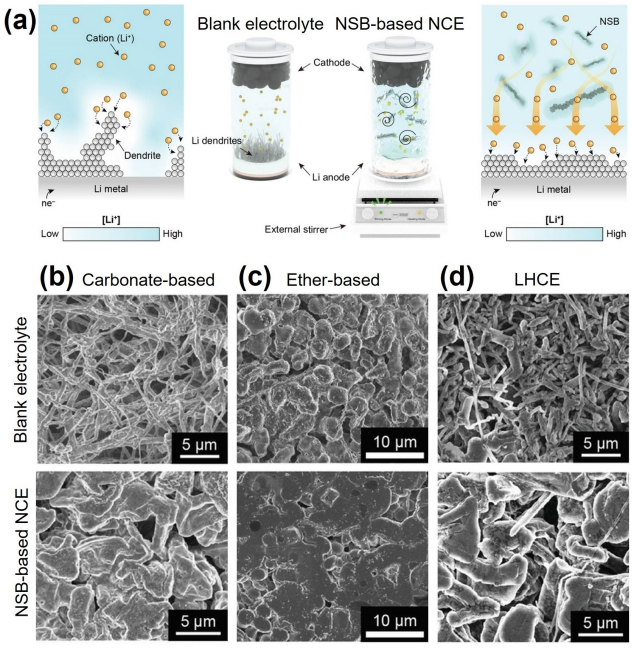

Figure 7. (a) Scheme of improved Li^+ transport through NSB-assisted convection. The versatility of NSB-assisted convective Li^+ transport in inhibiting the growth of Li dendrites using (b-d) carbonate-, ether-based electrolytes and LHCE. Reproduced from[70] Copyright (2022), with permission from Wiley-VCH.

5.2. Delivery of SEI-beneficial additives via nano-carrier role

Functional surface substituents on nanoparticles used in NCEs, endowing them with the role of nano-carriers, were introduced by Lee's research team.[51] Unlike common particles with –OH groups such as SiO_2, nano-carriers have citric acid (CA) as a functional group, offering abundant active sites compared to commercial nanoparticles (Figure 8a). The abundance of active sites allows them to capture anions and additives effectively. Indeed, ^{7}Li NMR analysis shows an upshift resulting from the strong Li-solvent interaction due to the anion-absorbing effect of the nano-carriers. Furthermore, the adsorption of anions and additives in the nano-carrier-based NCE was confirmed by the downfield shift in ^{19}F NMR spectrum (Figure 8b). These effects were further corroborated by the highly solvent-separated ion pair and coordinated FEC observed in the Raman spectra (Figure 8c). This enhanced selective Li^+ transport enhances the Li-deposited morphology. A comparison of the Li morphology achieved using blank electrolytes, moderate SiO_2-based NCEs (SCE), and CA-SiO_2-based NCEs (C-SCE) validated the compact shape of C-SCE (Figures 8d–f). In addition, nano-carriers modify the Li microenvironment within the electrolyte and simultaneously transport anions and additives to the LMA, thereby modifying the SEI. A comparison of the thickness of the SEIs formed in each electrolyte using cryo-TEM confirmed that C-SCE exhibited a thinner SEI layer than the blank and SCE.

Securing the long-term stability of NCE is essential to maintain its beneficial roles in stabilizing LMAs during prolonged cycling. As is well-established in the field of colloid engineering, the choice of solvent, Li salt, and their composition can customize the ionic strength of the surrounding electrolyte solutions,[94] balancing the electrostatic nature of nanoparticles. Moreover, the size and geometry of nanoparticles can also influence the overall charge balance of NCEs by regulating the active surface area interacting with electrolyte species.[52,69] In addition to nanoparticle design and dispersing medium, the selection of surface coatings and functional groups on nanoparticles

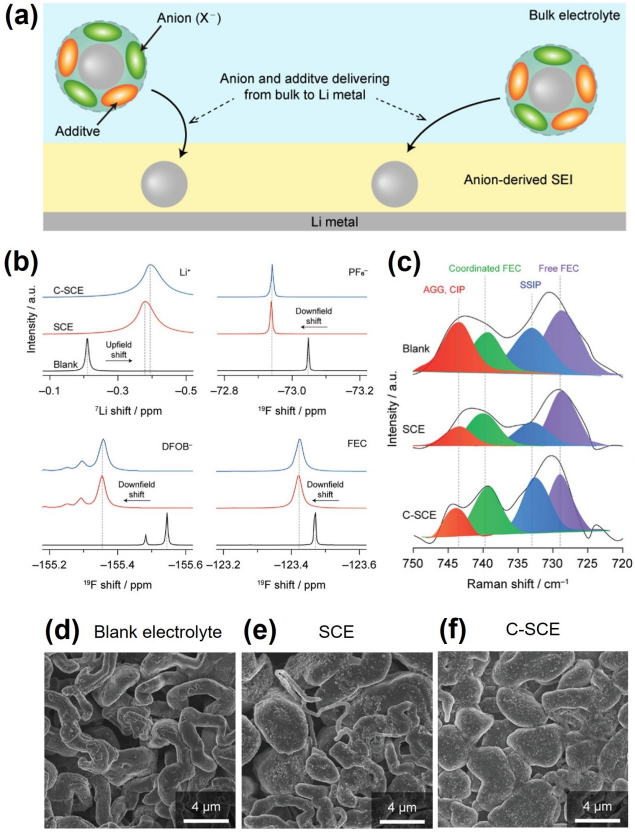

Figure 8. (a) Scheme of nano-carriers modifying Li^+ microenvironment and SEI chemistry. (b) Chemical shifts of ^7Li and ^{19}F NMR in various electrolytes caused by Li^+, PF_6^-, difluoro(ethanedioato)borate ion ($DFOB^-$), and FEC. Investigation using Raman spectroscopy into the solvation structure of the electrolytes and the molar fractions of (c) aggregates (AGGs), contact ion pairs (CIPs) compared to solvent-separated ion pairs (SSIPs), and coordinated FEC vs. unbound FEC. (d–f) SEM images of blank electrolyte, SCE, and C-SCE using Li||Cu asymmetric cells at 0.5 mA cm^{-2}, 1.0 mAh cm^{-2}. Reproduced from[51] Copyright (2023), with permission from Wiley-VCH.

profoundly impacts their interactions.[54,55] Some functional groups, such as polymers or surfactants, can induce steric or electrostatic repulsion, effectively preventing nanoparticles from coming into close contact and forming aggregates. Alternatively, introducing an anti-aggregation agent or surfactant into the NCEs can help mitigate aggregation or sedimentation. Unfortunately, most additives can be decomposed by parasitic reactions with LMAs, which can adversely affect the SEI stability. Therefore, there is an urgent need to search for electrochemically inert dispersants or surfactants, thereby ensuring long-term stability and consistent improvement in LMB performances.

6. Conclusion and Perspectives

In this review, we explored various NCEs to tailor the Li^+ microenvironment and Li-electrolyte interface chemistry to inhibit Li dendrite growth and enhance the LMB performances. Although it is not fully clarified which electrolyte species the nanoparticles bind with, they affect the Li^+ coordinating nature upon Li^+ transfer and SEI formation. Notably, restricting the anion mobility using nanoparticles enables Li^+ selective transfer, which is beneficial to suppress Li dendrite formation based on the Chazalviel diffusion model. Indeed, many cases have demonstrated high t_{Li+} when incorporating the nanoparticles. Inhibition of dendritic Li plating can alleviate the extensive side reactions with electrolytes, stabilizing the LMA surface. Aside from the "diffusion-controlled" Li dendrite inhibition, nanoparticles can modify the Li^+ solvation structures in the liquid electrolytes, tailoring SEI-forming reaction routes and ultimately promoting anion-derived, fluorinated SEI buildup. Although they cannot directly participate in the SEI-forming reactions, physically co-depositing the nanoparticles can help reinforce the mechanical stability of the SEI. For instance, chemically stable nanodiamonds, nanolithia (Li_2O), and LiF nanobox can inevitably undergo physical precipitation upon Li electroplating. Also, high-modulus BNNS can firmly adhere to Li deposits, mechanically suppressing Li dendrite growth. In contrast, oxide-based nanoparticles like SiO_2, Al_2O_3, and MOF may permit direct chemical reactions with LMA, yielding compounds like Li_xSiO_y, $Li_xAl_yO_z$, and derivatives, partially contribute to "SEI-controlled" LMA stabilization.

Table 1 provides a summary of various nano-materials, their compositions, and their different working mechanisms for suppressing Li dendrites. Despite their promises in performance enhancement, NCE approaches pose challenges, particularly within practical cell platforms, such as constrained electrolyte amounts and highly stacked cell configurations. Large nanoparticles (> 500 nm) may not permeate the separator pores, hindering physical access toward the LMAs and/or the electrode layers. Even though the nanoparticles were well-dispersed in the electrolytes, this adversely leads to poor dispersion within the cells during electrolyte injection. Moreover, the pore-clogging of the separators by nanoparticles can adversely affect Li^+ transport and deteriorate the Li^+ flux distribution. Moreover, NCEs may inevitably enhance the viscosity. In this regard, NCEs should provide their beneficial roles even at lower nanoparticle concentrations without compromising the electrolyte viscosity. Considering that colloidal stability against aggregation and sedimentation is crucial for maintaining their performance, the dispersion properties and long-term stability of NCEs should be enhanced by incorporating carefully designed nanoparticles, chemically/electrochemically inert dispersing agents, size-regulated anions, controlled surface charges, and functional groups. By addressing the above issues, we believe that NCE approach can extend its role beyond simply enhancing the performance of LMBs to enable the design of smart-battery electrolytes. Exploiting nano-encapsulation of functional materials, such as flame retardant, self-extinguishing, and Li-leaching agents, offers the potential to enhance battery safety significantly. Moreover, fluorescent nanoparticles with Li^+ binding features may enable the tracking of Li^+ movement,

Table 1. Summaries of the other relevant studies about LMB full cell cycle performance using NCE consisting of enhancement mechanism, materials, electrolyte composition, cycle condition, cathode, Li metal thickness, capacity, and retention.

Working mechanism	Materials (size)	Electrolyte composition (amount)	Cycle condition	Cathode	Li metal thickness	Capacity (cycle, retention)	Ref
Li microenvironment modulation	MOF (500 nm)	1 M $LiPF_6$ in EC/DEC (100 μL)	C/3, C/3	NMC	50 μm	3.3 mAh cm^{-2} (200th, 83%)	[59]
	BNNS (Lateral:1.5 μm, Thick: 4.5 nm)	1 M LiTFSI in DOL/DME (1:1 vol%) + 2 wt% $LiNO_3$ (60 μL)	C/5, C/5	Sulfur	Uninformed	1.8 mAh cm^{-2} (200th, 84%)	[60]
	Nanodiamond (5 nm)	1 M $LiPF_6$ in EC/DEC (uninformed)	1 C, 1 C	LFP	1.0 mm	Uninformed (190th, 70%)	[66]
SEI modulation	SiO_2 (13 nm)	1 M $LiPF_6$ in EC/DEC (1:1 vol%) + 5 wt% FEC (uninformed)	1 C, 1 C	NMC622	Thick	2.0 mAh cm^{-2} (170th, 70%)	[68]
	LiF nanobox (150 nm)	1 M $LiPF_6$/0.05 M LiDFOB in EC/DMC/DEC/FEC (28:28:28:16 vol%) (uninformed)	1 C, 1 C	NMC811	Thick	4.3 mAh cm^{-2} (200th, 87%)	[69]
Li microenvironment & SEI modulation	Li_2O (90 nm)	1 M LiFSI in FDMB (3.0 g/Ah)	C/5, C/2	NMC811	Cu	4.0 mAh cm^{-2} (70th, 65%)	[52]
	Li_3N (90 nm)	1 M $LiPF_6$ in EC/DEC (1:1 vol%) + 10 vol% FEC (20 μL)	C/2, 1 C	NMC811	750 μm	4.0 mAh cm^{-2} (140th, 93%)	[64]
	SiO_2 (7 nm)	1 M $LiPF_6$ in EC/EMC (30:70 wt%) + 2 wt% VC (75 μL)	C/5, C/2	NMC811	40 μm	4.2 mAh cm^{-2} (100th, 70%)	[63]
Mesoscale turbulence inducement	Nanospinbar (length: 1 μm, Diameter: 100 nm)	LiFSI:1.2 DME:3 TTE (200 μL)	1 C, 1 C	NMC622	50 μm	1.7 mAh cm^{-2} (600th, 70%)	[70]
Additive delivery	Citric acid-treated SiO_2 (7 nm)	0.6 M $LiPF_6$/0.6 M LiDFOB in FEC/DEC (1:2 vol%) (6.0 g/Ah)	C/5, C/2	NCA	50 μm	4.8 mAh cm^{-2} (110th, 70%)	[51]

thus facilitating an in-depth analysis of the electrochemical reaction mechanisms.

Keywords: Electrochemistry · Electrolytes · Lithium Metal Battery · Nano-Colloidal Electrolytes · Nanoparticles

Acknowledgements

This research was supported by the National Research Foundation (NRF) of Korea through Excellent Young Scientist Program (2020R1 C1 C1009159) and Engineering Research Center of Excellence Program (RS-2023-00222166) funded by the Ministry of Science and ICT (MSIT). H. Lee especially thanks to the support from the Brain Korea 21 FOUR Program at DGIST.

Conflict of Interests

The authors declare no conflict of interest.

Data Availability Statement

This article doesn't involve data sharing since there was no generation or analysis of new data in this study.

[1] J. M. Tarascon, M. Armand, *Nature* **2001**, *414*, 359–367.
[2] J. B. Goodenough, K.-S. Park, *J. Am. Chem. Soc.* **2013**, *135*, 1167–1176.
[3] B. Dunn, H. Kamath, J.-M. Tarascon, *Science* **2011**, *334*, 928–935.
[4] M. S. Whittingham, *Chem. Rev.* **2014**, *114*, 11414–11443.
[5] P. Albertus, S. Babinec, S. Litzelman, A. Newman, *Nat. Energy* **2018**, *3*, 16–21.
[6] X.-B. Cheng, R. Zhang, C.-Z. Zhao, Q. Zhang, *Chem. Rev.* **2017**, *117*, 10403–10473.
[7] W. Xu, J. Wang, F. Ding, X. Chen, E. Nasybulin, Y. Zhang, J.-G. Zhang, *Energy Environ. Sci.* **2014**, *7*, 513–537.
[8] D. Jin, Y. Roh, T. Jo, M.-H. Ryou, H. Lee, Y. M. Lee, *Adv. Energy Mater.* **2021**, *11*, 2003769.
[9] D. Aurbach, E. Zinigrad, Y. Cohen, H. Teller, *Solid State Ionics* **2002**, *148*, 405–416.
[10] C. Niu, H. Lee, S. Chen, Q. Li, J. Du, W. Xu, J.-G. Zhang, M. S. Whittingham, J. Xiao, J. Liu, *Nat. Energy* **2019**, *4*, 551–559.
[11] J. Seo, W. Jeong, M. Lim, B. Choi, S. Park, Y. Jo, J.-W. Lee, H. Lee, *Energy Storage Mater.* **2023**, *60*, 102827.
[12] D. Lin, Y. Liu, Y. Cui, *Nat. Nanotechnol.* **2017**, *12*, 194–206.
[13] J. N. Chazalviel, *Phys. Rev. A* **1990**, *42*, 7355–7367.
[14] P. Bai, J. Li, F. R. Brushett, M. Z. Bazant, *Energy Environ. Sci.* **2016**, *9*, 3221–3229.
[15] C. Monroe, J. Newman, *J. Electrochem. Soc.* **2005**, *152*, A396.
[16] S.-G. Woo, E.-K. Hwang, H.-K. Kang, H. Lee, J.-N. Lee, H.-s. Kim, G. Jeong, D.-J. Yoo, J. Lee, S. Kim, J.-S. Yu, J. W. Choi, *Energy Environ. Sci.* **2021**, *14*, 1420–1428.

[17] R. Zahn, M. F. Lagadec, M. Hess, V. Wood, *ACS Appl. Mater. Interfaces* **2016**, *8*, 32637–32642.
[18] X. Mao, L. Shi, H. Zhang, Z. Wang, J. Zhu, Z. Qiu, Y. Zhao, M. Zhang, S. Yuan, *J. Power Sources* **2017**, *342*, 816–824.
[19] N.-W. Li, Y.-X. Yin, C.-P. Yang, Y.-G. Guo, *Adv. Mater.* **2016**, *28*, 1853–1858.
[20] Y. Liu, D. Lin, P. Y. Yuen, K. Liu, J. Xie, R. H. Dauskardt, Y. Cui, *Adv. Mater.* **2017**, *29*, 1605531.
[21] R. Pathak, K. Chen, A. Gurung, K. M. Reza, B. Bahrami, J. Pokharel, A. Baniya, W. He, F. Wu, Y. Zhou, K. Xu, Q. Qiao, *Nat. Commun.* **2020**, *11*, 93.
[22] L. Ma, C. Fu, L. Li, K. S. Mayilvahanan, T. Watkins, B. R. Perdue, K. R. Zavadil, B. A. Helms, *Nano Lett.* **2019**, *19*, 1387–1394.
[23] H. Lee, D. J. Lee, Y.-J. Kim, J.-K. Park, H.-T. Kim, *J. Power Sources* **2015**, *284*, 103–108.
[24] E. Cha, M. D. Patel, J. Park, J. Hwang, V. Prasad, K. Cho, W. Choi, *Nat. Nanotechnol.* **2018**, *13*, 337–344.
[25] R. Xu, X.-Q. Zhang, X.-B. Cheng, H.-J. Peng, C.-Z. Zhao, C. Yan, J.-Q. Huang, *Adv. Funct. Mater.* **2018**, *28*, 1705838.
[26] J. Wang, J. Yang, Q. Xiao, J. Zhang, T. Li, L. Jia, Z. Wang, S. Cheng, L. Li, M. Liu, H. Liu, H. Lin, Y. Zhang, *Adv. Funct. Mater.* **2021**, *31*, 2007434.
[27] Y. Sun, Y. Zhao, J. Wang, J. Liang, C. Wang, Q. Sun, X. Lin, K. R. Adair, J. Luo, D. Wang, R. Li, M. Cai, T.-K. Sham, X. Sun, *Adv. Mater.* **2019**, *31*, 1806541.
[28] P. Matteo, T. Akiko, A. Henry, N. Maria Assunta, P. Stefano, *Energy Mater.* **2023**, *3*, 300049.
[29] S. Junli, N. Huu-Dat, C. Zhen, W. Rui, S. Dominik, B. Lester, L. Jie, F. Henrich, B. Dominic, I. Cristina, P. Elie, *Energy Mater.* **2023**, *3*, 300036.
[30] Q. Zhou, X. Yang, X. Xiong, Q. Zhang, B. Peng, Y. Chen, Z. Wang, L. Fu, Y. Wu, *Adv. Energy Mater.* **2022**, *12*, 2201991.
[31] L. Zhang, M. Ling, J. Feng, L. Mai, G. Liu, J. Guo, *Energy Storage Mater.* **2018**, *11*, 24–29.
[32] X.-Q. Zhang, X.-B. Cheng, X. Chen, C. Yan, Q. Zhang, *Adv. Funct. Mater.* **2017**, *27*, 1605989.
[33] T. Hou, G. Yang, N. N. Rajput, J. Self, S.-W. Park, J. Nanda, K. A. Persson, *Nano Energy* **2019**, *64*, 103881.
[34] D. Kang, D. Jin, J. Moon, C. B. Dzakpasu, H. Lee, S. Choi, T. Jo, H. Lee, S.-Y. Ryou, Y. M. Lee, *Chem. Eng. J.* **2023**, *452*, 139409.
[35] X. Ren, L. Zou, X. Cao, M. H. Engelhard, W. Liu, S. D. Burton, H. Lee, C. Niu, B. E. Matthews, Z. Zhu, C. Wang, B. W. Arey, J. Xiao, J. Liu, J.-G. Zhang, W. Xu, *Joule* **2019**, *3*, 1662–1676.
[36] J. Qian, W. A. Henderson, W. Xu, P. Bhattacharya, M. Engelhard, O. Borodin, J.-G. Zhang, *Nat. Commun.* **2015**, *6*, 6362.
[37] X. Ren, S. Chen, H. Lee, D. Mei, M. H. Engelhard, S. D. Burton, W. Zhao, J. Zheng, Q. Li, M. S. Ding, M. Schroeder, J. Alvarado, K. Xu, Y. S. Meng, J. Liu, J.-G. Zhang, W. Xu, *Chem* **2018**, *4*, 1877–1892.
[38] Y. Chen, Z. Yu, P. Rudnicki, H. Gong, Z. Huang, S. C. Kim, J.-C. Lai, X. Kong, J. Qin, Y. Cui, Z. Bao, *J. Am. Chem. Soc.* **2021**, *143*, 18703–18713.
[39] C. V. Amanchukwu, Z. Yu, X. Kong, J. Qin, Y. Cui, Z. Bao, *J. Am. Chem. Soc.* **2020**, *142*, 7393–7403.
[40] Z. Yu, P. E. Rudnicki, Z. Zhang, Z. Huang, H. Celik, S. T. Oyakhire, Y. Chen, X. Kong, S. C. Kim, X. Xiao, H. Wang, Y. Zheng, G. A. Kamat, M. S. Kim, S. F. Bent, J. Qin, Y. Cui, Z. Bao, *Nat. Energy* **2022**, *7*, 94–106.
[41] Z. Yu, H. Wang, X. Kong, W. Huang, Y. Tsao, D. G. Mackanic, K. Wang, X. Wang, W. Huang, S. Choudhury, Y. Zheng, C. V. Amanchukwu, S. T. Hung, Y. Ma, E. G. Lomeli, J. Qin, Y. Cui, Z. Bao, *Nat. Energy* **2020**, *5*, 526–533.
[42] J. Xiao, *Science* **2019**, *366*, 426–427.
[43] W. Liu, D. Lin, A. Pei, Y. Cui, *J. Am. Chem. Soc.* **2016**, *138*, 15443–15450.
[44] Y. Yamada, A. Yamada, *J. Electrochem. Soc.* **2015**, *162*, A2406.
[45] Z. Yu, Y. Cui, Z. Bao, *Cell Rep. Phys. Sci.* **2020**, *1*, 100119.
[46] Z. Wang, F. Qi, L. Yin, Y. Shi, C. Sun, B. An, H.-M. Cheng, F. Li, *Adv. Energy Mater.* **2020**, *10*, 1903843.
[47] A. C. Balazs, T. Emrick, T. P. Russell, *Science* **2006**, *314*, 1107–1110.
[48] W. Liu, N. Liu, J. Sun, P.-C. Hsu, Y. Li, H.-W. Lee, Y. Cui, *Nano Lett.* **2015**, *15*, 2740–2745.
[49] L. Chen, Y. Li, S.-P. Li, L.-Z. Fan, C.-W. Nan, J. B. Goodenough, *Nano Energy* **2018**, *46*, 176–184.
[50] S. Choudhury, A. Agrawal, S. Wei, E. Jeng, L. A. Archer, *Chem. Mater.* **2016**, *28*, 2147–2157.
[51] M. Lim, H. An, J. Seo, M. Lee, H. Lee, H. Kwon, H.-T. Kim, D. Esken, R. Takata, H. A. Song, H. Lee, *Small* **2023**, *n/a*, 2302722.
[52] M. S. Kim, Z. Zhang, P. E. Rudnicki, Z. Yu, J. Wang, H. Wang, S. T. Oyakhire, Y. Chen, S. C. Kim, W. Zhang, D. T. Boyle, X. Kong, R. Xu, Z. Huang, W. Huang, S. F. Bent, L.-W. Wang, J. Qin, Z. Bao, Y. Cui, *Nat. Mater.* **2022**, *21*, 445–454.
[53] C. Pfaffenhuber, M. Göbel, J. Popovic, J. Maier, *Phys. Chem. Chem. Phys.* **2013**, *15*, 18318–18335.
[54] A. J. Bhattacharyya, *J. Phys. Chem. Lett.* **2012**, *3*, 744–750.
[55] S. K. Das, A. J. Bhattacharyya, *J. Phys. Chem. B* **2010**, *114*, 6830–6835.
[56] A. Jarosik, S. Hore, N. Kaskhedikar, C. Pfaffenhuber, J. Maier, *Electrochim. Acta* **2011**, *56*, 8115–8121.
[57] Y. Lu, S. K. Das, S. S. Moganty, L. A. Archer, *Adv. Mater.* **2012**, *24*, 4430–4435.
[58] A. J. Bhattacharyya, J. Maier, *Adv. Mater.* **2004**, *16*, 811–814.
[59] L. Shen, H. B. Wu, F. Liu, J. Shen, R. Mo, G. Chen, G. Tan, J. Chen, X. Kong, X. Lu, Y. Peng, J. Zhu, G. Wang, Y. Lu, *Adv. Funct. Mater.* **2020**, *30*, 2003055.
[60] J. Wu, X. Li, Z. Rao, X. Xu, Z. Cheng, Y. Liao, L. Yuan, X. Xie, Z. Li, Y. Huang, *Nano Energy* **2020**, *72*, 104725.
[61] C.-Z. Zhao, X.-Q. Zhang, X.-B. Cheng, R. Zhang, R. Xu, P.-Y. Chen, H.-J. Peng, J.-Q. Huang, Q. Zhang, *Proc. Natl. Acad. Sci. USA* **2017**, *114*, 11069–11074.
[62] H. Xu, Y. He, Z. Zhang, J. Shi, P. Liu, Z. Tian, K. Luo, X. Zhang, S. Liang, Z. Liu, *J. Energy Chem.* **2020**, *48*, 375–382.
[63] J. Lee, H.-S. Lim, X. Cao, X. Ren, W.-J. Kwak, I. A. Rodríguez-Pérez, J.-G. Zhang, H. Lee, H.-T. Kim, *ACS Appl. Mater. Interfaces* **2020**, *12*, 37188–37196.
[64] M. S. Kim, Z. Zhang, J. Wang, S. T. Oyakhire, S. C. Kim, Z. Yu, Y. Chen, D. T. Boyle, Y. Ye, Z. Huang, W. Zhang, R. Xu, P. Sayavong, S. F. Bent, J. Qin, Z. Bao, Y. Cui, *ACS Nano* **2023**, *17*, 3168–3180.
[65] Y. Liao, L. Yuan, X. Liu, J. Meng, W. Zhang, Z. Li, Y. Huang, *Energy Storage Mater.* **2022**, *48*, 366–374.
[66] X.-B. Cheng, M.-Q. Zhao, C. Chen, A. Pentecost, K. Maleski, T. Mathis, X.-Q. Zhang, Q. Zhang, J. Jiang, Y. Gogotsi, *Nat. Commun.* **2017**, *8*, 336.
[67] W. Chen, Y. Hu, W. Lv, T. Lei, X. Wang, Z. Li, M. Zhang, J. Huang, X. Du, Y. Yan, W. He, C. Liu, M. Liao, W. Zhang, J. Xiong, C. Yan, *Nat. Commun.* **2019**, *10*, 4973.
[68] M. Kim, Y. Jeon, Y.-G. Cho, H.-K. Song, *J. Power Sources* **2019**, *414*, 218–224.
[69] Y.-H. Tan, G.-X. Lu, J.-H. Zheng, F. Zhou, M. Chen, T. Ma, L.-L. Lu, Y.-H. Song, Y. Guan, J. Wang, Z. Liang, W.-S. Xu, Y. Zhang, X. Tao, H.-B. Yao, *Adv. Mater.* **2021**, *33*, 2102134.
[70] M. Lim, S. Kim, J. Kang, D. Jin, H. An, H. Lee, J. Park, M. Lee, J. Seo, H. Lee, Y. M. Lee, H. Lee, *Adv. Funct. Mater.* **2022**, *32*, 2204052.
[71] N. Sun, R. Li, Y. Zhao, H. Zhang, J. Chen, J. Xu, Z. Li, X. Fan, X. Yao, Z. Peng, *Adv. Energy Mater.* **2022**, *12*, 2200621.
[72] Y. Zou, F. Cheng, Y. Lu, Y. Xu, C. Fang, J. Han, *Small* **2023**, *19*, 2203394.
[73] Y. Zhou, X. Zhang, Y. Ding, J. Bae, X. Guo, Y. Zhao, G. Yu, *Adv. Mater.* **2020**, *32*, 2003920.
[74] X. Li, Z. Chu, H. Jiang, Y. Dai, W. Zheng, A. Liu, X. Jiang, G. He, *Energy Storage Mater.* **2021**, *37*, 233–242.
[75] G. A. Giffin, A. Moretti, S. Jeong, S. Passerini, *J. Power Sources* **2017**, *342*, 335–341.
[76] X. Shen, J. Zhang, H. Chen, H. Sun, L. Zhang, B. Li, H. Zhang, X. Li, S. Li, J. Zhu, X. Duan, *Energy Storage Mater.* **2023**, *61*, 102878.
[77] X.-B. Cheng, C. Yan, H.-J. Peng, J.-Q. Huang, S.-T. Yang, Q. Zhang, *Energy Storage Mater.* **2018**, *10*, 199–205.
[78] J. Chen, Q. Li, T. P. Pollard, X. Fan, O. Borodin, C. Wang, *Mater. Today* **2020**, *39*, 118–126.
[79] J. Wu, Z. Rao, X. Liu, Y. Shen, C. Fang, L. Yuan, Z. Li, W. Zhang, X. Xie, Y. Huang, *Adv. Mater.* **2021**, *33*, 2007428.
[80] L. Liu, J. Wang, *Nano Lett.* **2023**.
[81] M. Baek, J. Kim, K. Jeong, S. Yang, H. Kim, J. Lee, M. Kim, K. J. Kim, J. W. Choi, *Nat. Commun.* **2023**, *14*, 1296.
[82] M. He, R. Guo, G. M. Hobold, H. Gao, B. M. Gallant, *Proc. Natl. Acad. Sci. USA* **2020**, *117*, 73–79.
[83] J. Zhao, L. Liao, F. Shi, T. Lei, G. Chen, A. Pei, J. Sun, K. Yan, G. Zhou, J. Xie, C. Liu, Y. Li, Z. Liang, Z. Bao, Y. Cui, *J. Am. Chem. Soc.* **2017**, *139*, 11550–11558.
[84] W. Tang, X. Yin, Z. Chen, W. Fu, K. P. Loh, G. W. Zheng, *Energy Storage Mater.* **2018**, *14*, 289–296.
[85] T. T. Beyene, H. K. Bezabh, M. A. Weret, T. M. Hagos, C.-J. Huang, C.-H. Wang, W.-N. Su, H. Dai, B.-J. Hwang, *J. Electrochem. Soc.* **2019**, *166*, A1501.
[86] Q. Sun, S. Wang, Y. Ma, Y. Zhou, D. Song, H. Zhang, X. Shi, C. Li, L. Zhang, *Energy Storage Mater.* **2022**, *44*, 537–546.
[87] Z. Wang, H. Zhang, J. Xu, A. Pan, F. Zhang, L. Wang, R. Han, J. Hu, M. Liu, X. Wu, *Adv. Funct. Mater.* **2022**, *32*, 2112598.

[88] Y. Zhao, D. Wang, Y. Gao, T. Chen, Q. Huang, D. Wang, *Nano Energy* **2019**, *64*, 103893.
[89] X. Peng, Y. Lin, Y. Wang, Y. Li, T. Zhao, *Nano Energy* **2022**, *96*, 107102.
[90] D. V. Novikov, E. Y. Evschik, V. I. Berestenko, T. V. Yaroslavtseva, A. V. Levchenko, M. V. Kuznetsov, N. G. Bukun, O. V. Bushkova, Y. A. Dobrovolsky, *Electrochim. Acta* **2016**, *208*, 109–119.
[91] C. K. Chan, H. Peng, G. Liu, K. Mcllwrath, X. F. Zhang, R. A. Huggins, Y. Cui, *Nat. Nanotechnol.* **2008**, *3*, 31–35.
[92] T. Yim, M.-S. Park, S.-G. Woo, H.-K. Kwon, J.-K. Yoo, Y. S. Jung, K. J. Kim, J.-S. Yu, Y.-J. Kim, *Nano Lett.* **2015**, *15*, 5059–5067.
[93] M. Baginska, N. R. Sottos, S. R. White, *ACS Omega* **2018**, *3*, 1609–1613.
[94] N. Kaskhedikar, Y. Karatas, G. Cui, J. Maier, H. D. Wiemhöfer, *J. Mater. Chem.* **2011**, *21*, 11838–11843.

Manuscript received: October 31, 2023
Revised manuscript received: January 8, 2024
Version of record online: January 26, 2024